

Mössbauer Emission Spectroscopy of ^{57}Fe Arising from ^{57}Mn in Metal and Oxides of Chromium

M. NAKADA, Y. WATANABE, K. ENDO, H. NAKAHARA, H. SANO, K. MISHIMA,[†] M. K. KUBO,[†]
Y. SAKAI,[†] T. TOMINAGA,[†] K. ASAI,^{††} M. IWAMOTO,^{†††} Y. KOBAYASHI,^{†††}
T. OKADA,^{†††} N. SAKAI,^{†††} I. KOHNO,^{†††} and F. AMBE^{†††,*}

Department of Chemistry, Faculty of Science, Tokyo Metropolitan University,
Hachioji, Tokyo 192-03

[†] Department of Chemistry, Faculty of Science, The University of Tokyo,
Bunkyo-ku, Tokyo 113

^{††} Department of Applied Physics and Chemistry, The University of Electro-
Communications, Chofu, Tokyo 182

^{†††} The Institute of Physical and Chemical Research (RIKEN), Wako, Saitama 351-01
(Received July 15, 1991)

The chemical states of ^{57}Fe arising from ^{57}Mn produced by the $^{54}\text{Cr}(\alpha, p)^{57}\text{Mn}$ reaction in the metal and oxides of chromium were studied by ^{57}Fe Mössbauer emission spectroscopy. In chromium metal, all of the ^{57}Fe atoms were found at substitutional sites. Both the iron(II) and iron(III) species were observed in Cr_2O_3 , while only iron(III) ions were detected in CrO_3 .

Mössbauer emission spectroscopy offers unique information concerning the site occupation and chemical states of extremely diluted impurity atoms in a solid. A large number of physical and chemical emission studies have been carried out concerning ^{57}Fe produced by the EC decay of ^{57}Co in various matrices. However, little attention has been paid to ^{57}Mn , another source nuclide of ^{57}Fe , since the pioneering work of Preston and Zabransky in 1975.¹⁾ The short-lived nuclide ^{57}Mn (1.45 min) undergoes β -decay, about 80% of it decaying directly to the 14.4 keV Mössbauer level of ^{57}Fe (Fig. 1).^{2,3)} In nonmetallic substances, EC decay is known to result in appreciable damage around the decaying atom due to an Auger process following the decay. In the case of β -decay, on the other hand, the aftereffects are generally not serious, and often an increase in the

oxidation number by one is observed, sometimes resulting in new chemical species.^{4–6)} Manganese can take oxidation states up to 7+ in ordinary solid state chemistry, which is not the case for cobalt. Therefore, different chemical states are expected for ^{57}Fe arising from ^{57}Mn , compared with that from ^{57}Co . Especially, iron species in an unusually high-oxidation state might be detected after the decay of ^{57}Mn in an appropriate matrix. So far as we know, there have been no investigations with such an object in view. In a search of the possibilities we initiated a series of studies on the chemical states of ^{57}Fe arising from ^{57}Mn . This paper describes an experimental device used to observe the Mössbauer emission spectra of the short-lived ^{57}Mn produced by the $^{54}\text{Cr}(\alpha, p)^{57}\text{Mn}$ reaction as well as the experimental results concerning Cr metal, Cr_2O_3 , and CrO_3 . The results are discussed in terms of the physicochemical properties of the matrices.

Experimental

Target Transportation System. A target transportation system was designed and constructed, which enables efficient Mössbauer spectroscopy of ^{57}Fe using short-lived source nuclide under a low γ -ray background. It was installed in a one-meter diameter scattering chamber at a beam course of the Riken 160 cm cyclotron. A plane figure of the system is shown in Fig. 2. A target (A) is irradiated at the center of the chamber with the cyclotron beam. After irradiation, a shutter installed in the far upper stream of the beam is closed so as to stop it, and the target is transported close to a side window of the chamber, as is denoted by A' in the figure, by means of a motor (B) and a drive wire (C) for the Mössbauer measurement. The time required for the transportation is about 10 s. When the measurement is finished, the target is moved back to the center of the chamber for further irradiation. The cycle of irradiation and measurement can be repeated, the time of both steps being selectable. The target is mounted on a graphite holder surface (D) slanted upwards at an angle of 45° against the beam in order to enlarge the target area. The holder is set

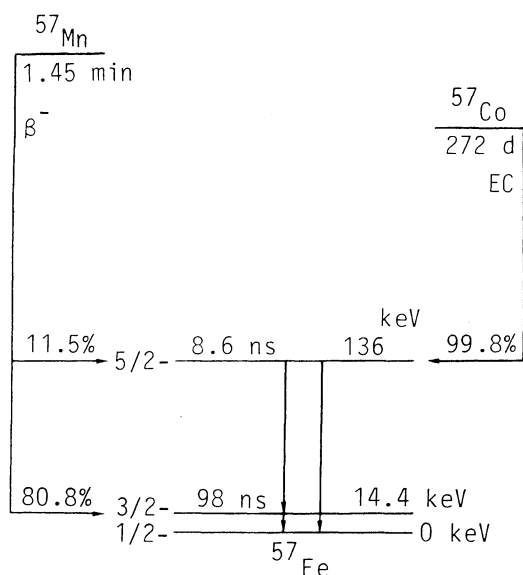


Fig. 1. Simplified decay scheme of ^{57}Mn and ^{57}Co . Minor branchings are not shown.

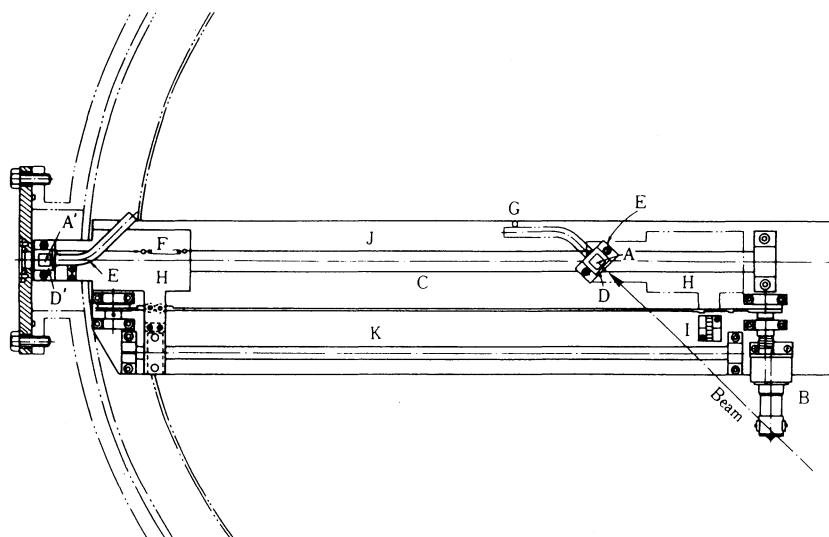


Fig. 2. Plane figure of the target transportation system. A: Target, B: motor, C: drive wire, D: target holder, E: target rotator, F: spring, G: pole, H: moving rack, I: limit switch, J: main rail, and K: subrail. The target and the target holder are shown in both positions of irradiation (A, D) and measurement (A', D'). The axis of rotation of the target rotator penetrates the center of the target area.

on a rotator (E) with a long bent tail. It can rotate around its central axis, but is strained in the clock-wise direction with a spring (F). So long as the target is at the center of the chamber, that is, in the position for the irradiation, the target is directed to the beam, rotation of the rotator being hindered by a pole (G). When the rotator moves toward the window on its rack (H), the tail of the rotator is released from the pole and the target turns so as to face the window due to the force of the spring. The system is expected to be useful also for the γ -ray spectroscopy of nuclides with a half-life exceeding several seconds, since the γ -ray background is considerably reduced in comparison with the usual on-line experiments.

Preparation of the Target Materials. Enriched ^{54}Cr metal and $^{54}\text{Cr}_2\text{O}_3$ (^{54}Cr 96.78%) were purchased from Oak Ridge National Laboratory. $^{54}\text{Cr}_2\text{O}_3$ was synthesized from $^{54}\text{Cr}_2\text{O}_3$ by the following procedure. $^{54}\text{Cr}_2\text{O}_3$ was fused with Na_2CO_3 in a platinum crucible. The product was dissolved in 6 mol dm^{-3} HCl solution. The solution was warmed for several hours to reduce $^{54}\text{Cr(VI)}$ to $^{54}\text{Cr}^{3+}$. A dilute NaOH solution was added to the solution in order to precipitate hydroxide of the trivalent chromium at pH 7–8. The hydroxide precipitate was thoroughly washed with water in order to remove Na^+ and Cl^- ions. $^{54}\text{Cr}^{3+}$ ions of the hydroxide were oxidized to $^{54}\text{Cr(VI)}$ by H_2O_2 . Excess H_2O_2 was decomposed by heating. The $^{54}\text{Cr(VI)}$ solution was finally evaporated at about 120°C to yield $^{54}\text{Cr}_2\text{O}_3$. The target materials were fixed on the graphite holder described above with a small amount of a cellulose or styrene-butadiene rubber binder. The area of the targets was about $6\text{ mm} \times 10\text{ mm}$ and the total amount was a few mg for metal and about 30 mg for the oxides.

Irradiation. The target was irradiated with 22 MeV α -particles accelerated by the cyclotron. The beam current was 150–300 nA. After 90 s of irradiation, the holder with the target was transported to the measurement position. The temperature of the target was observed to rise by a few tens of

degrees during the irradiation, but to be only several degrees higher than room temperature at the time of the Mössbauer measurement.

Mössbauer Measurement. Mössbauer measurements were performed using a transducer comprising two piezoelectric bimorph actuators, developed by one of the authors (N.S.).⁷⁾ A temperature-control system was installed in order to minimize the drift of the actuator during prolonged runs. An enriched stainless-steel absorber (310SS, 1.0 mg $^{57}\text{Fe}/\text{cm}^2$, $20\text{ mm} \times 20\text{ mm}$) was driven in a sinusoidal mode by the actuators. The 14.4 keV resonant γ -rays were detected with a $16\text{ mm} \phi \times 5\text{ mm}$ Si(Li) detector. A typical γ -ray spectrum is shown in Fig. 3. The half-life of the 14.4 keV peak was found to be $1.40 \pm 0.03\text{ min}$, in agreement with the literature value of

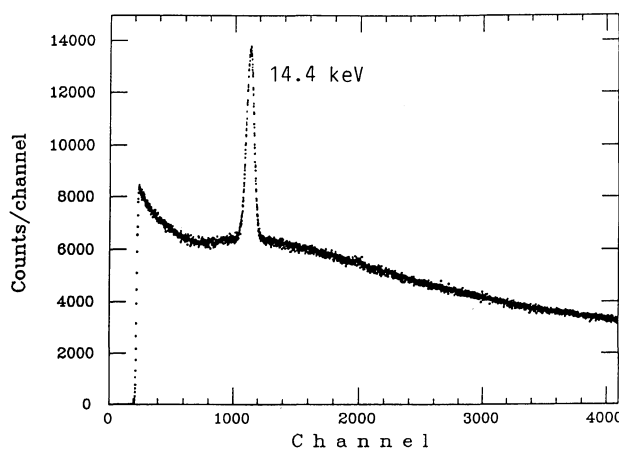


Fig. 3. Typical γ -ray spectrum of ^{57}Mn produced by the $^{54}\text{Cr}(\alpha, p)^{57}\text{Mn}$ reaction. Detector: $16\text{ mm} \phi \times 5\text{ mm}$ Si(Li).

1.45 min for ^{57}Mn .³⁾ The Mössbauer data were stored in the 1024-channel memory of a multichannel analyzer. The counting rate was 0.5–2 counts/(channel·min). After 90 s of measurement, the target was sent back to the center of the chamber to repeat the cycle: Irradiation of 90 s, transportation of 13 s, measurement of 90 s, and transportation of 13 s. A typical run continued for a few days. No appreciable ^{57}Co was detected, even after prolonged irradiation. The velocity calibration was carried out using a source of ^{57}Co embedded in iron foil.

Results and Discussion

The emission Mössbauer spectra of ^{57}Fe arising from

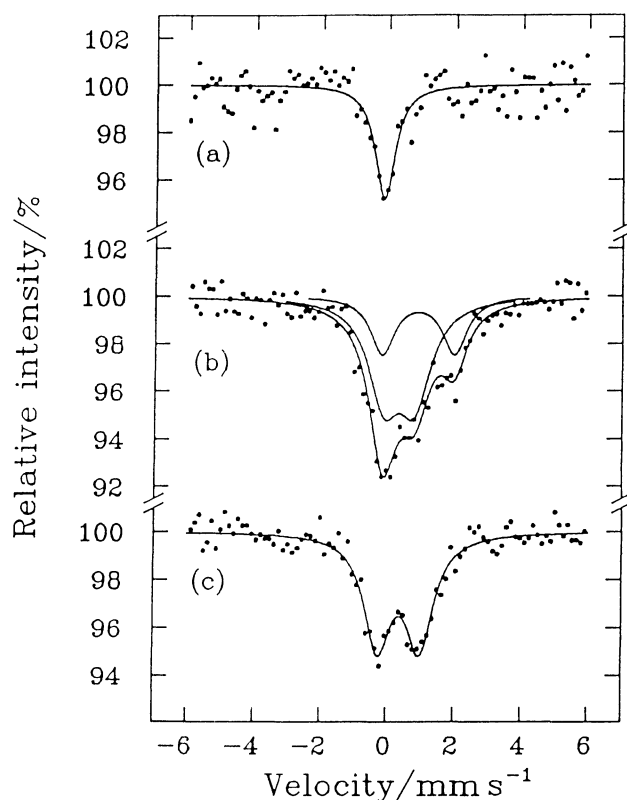


Fig. 4. Emission Mössbauer spectra of ^{57}Fe arising from ^{57}Mn produced by the $^{54}\text{Cr}(\alpha, p)^{57}\text{Mn}$ reaction in (a) ^{54}Cr metal, (b) $^{54}\text{Cr}_2\text{O}_3$, and (c) $^{54}\text{CrO}_3$. The number of counts at the baseline was about 24600, 42000, and 59600, respectively.

^{57}Mn in metal and the oxides of chromium are shown in Fig. 4. The isomer shift is given relative to iron metal at room temperature, and the sign is converted to be as in the usual absorption spectra. The numerical parameters determined by a least-squares fitting procedure assuming Lorentzian components are given in Table 1.

The large width of every peak is firstly attributed to the enriched stainless-steel absorber employed, which gives a full width at the half maximum of about 0.65 mm s^{-1} against a standard $^{57}\text{Co}/\text{Rh}$ source. To this, broadening due to defects created by the nuclear reaction and the β -decay is considered to be superposed.

The emission spectrum of ^{57}Mn in chromium metal (Fig. 4(a)) consists of a singlet with an isomer shift of -0.14 mm s^{-1} . The value is in good agreement with that of ^{57}Co doped in chromium metal.⁸⁾ This observation shows that all of the ^{57}Fe atoms arising from ^{57}Mn occupy the substitutional sites in the chromium metal matrix at the time of the Mössbauer measurement, though the (α , p) reaction and a part of the β -decay impart sufficient energy to displace the resulting nuclei from the original sites. The behavior of energetic atoms in metals has been extensively studied by Mössbauer measurements on atoms implanted by acceleration and Coulomb excitation.⁹⁾ In metals, the implanted atoms almost always substitute atoms of the host lattice, though they are often partly associated with vacancies created by the implantation process. If the impurity atoms have any degree of solubility in the host, these vacancies become dissociated from them when annealed at a sufficiently high temperature.⁹⁾ The above observation concerning ^{57}Mn in chromium metal indicates that the defect structures formed around ^{57}Mn as a result of recoil following the nuclear reaction were completely annealed before the Mössbauer measurement on its daughter ^{57}Fe .

In the case of Cr_2O_3 , two quadrupole doublets were identified, as can be seen in Fig. 4(b). A doublet with a smaller isomer shift is assigned to high-spin iron(III) species on the basis of the isomer shift, while the other is assigned to high-spin iron(II) species. Chromium(III) oxide is isomorphous with corundum¹⁰⁾ and is anti-ferromagnetically ordered below the Néel temperature of 307 K .¹¹⁾ Since the Mössbauer measurement was made at about 30°C , the matrix is estimated to have had little magnetization. This is consistent with the absence of

Table 1. Mössbauer Parameters of ^{57}Fe Arising from ^{57}Mn Produced by the $^{54}\text{Cr}(\alpha, p)^{57}\text{Mn}$ Reaction in Metal and Oxides of Chromium at 300 K

Sample	Isomer shift ^{a)} mm s^{-1}	Quadrupole splitting mm s^{-1}	Width ^{b)} mm s^{-1}	Relative area %
^{54}Cr metal	-0.14 ± 0.04		0.74 ± 0.11	100
$^{54}\text{Cr}_2\text{O}_3$	0.34 ± 0.07	0.92 ± 0.13	1.18 ± 0.26	68 ± 2 32 ± 9
	0.90 ± 0.12	2.15 ± 0.23	0.89 ± 0.24	
$^{54}\text{CrO}_3$	0.37 ± 0.02	1.26 ± 0.04	1.00 ± 0.06	100

a) Relative to metallic iron at room temperature. b) Full width at the half maximum.

magnetic components in the observed spectrum.

Preston and Zabransky observed a broad single peak of Fe^{3+} along with a doublet assigned to Fe^{2+} at room temperature in their earlier work on ^{57}Mn in Cr_2O_3 .¹⁾ The relative area of the iron(II) doublet in their spectrum is much smaller than that in ours, though the values of the isomer shift and quadrupole splitting are in good agreement. The observed differences are ascribed to differences in the experimental conditions, such as the particle size of the sample and time sequence of irradiation and measurement.

The isomer shift of the iron(III) doublet observed in the present work is essentially the same as that of the iron(III) ions in $\alpha\text{-Fe}_2\text{O}_3$,^{12,13)} which has the same corundum-type crystal structure¹⁴⁾ as Cr_2O_3 . Therefore, the iron(III) doublet is ascribed to ions substituted for the chromium ions in Cr_2O_3 . The observed quadrupole splitting, $2e^2qQ$, of the doublet, however, is much larger than that of $^{57}\text{Fe}^{3+}$ ions dilutely doped in Cr_2O_3 (0.26 mm s^{-1} at 330 K),¹⁵⁾ as well as that of paramagnetic $\alpha\text{-Fe}_2\text{O}_3$ (0.49 mm s^{-1} above the Néel temperature of 955 K).¹⁶⁾ This difference is ascribed to a defect structure near the $^{57}\text{Fe}^{3+}$ atoms arising from ^{57}Mn in the insulating matrix of Cr_2O_3 , where defects are less easily restorable than in metals.⁹⁾ Manganese ions are reported to replace the iron(III) ions of $\alpha\text{-Fe}_2\text{O}_3$,¹⁷⁾ though their valence state was not determined. Similarly, ^{57}Mn ions are considered to occupy the Cr site in Cr_2O_3 . However, they are not necessarily in the trivalent state. This is one possible origin of the defect structure near the $^{57}\text{Fe}^{3+}$ arising from them.

The isomer shift of the iron(II) fraction of ^{57}Fe atoms in Cr_2O_3 is comparable to those of the iron(II) components of Fe_{1-x}O (wüstite), whereas the quadrupole splitting of the former is far larger than those of the latter.¹⁸⁾ The iron(II) doublet observed is most probably ascribed to iron(II) ions at the Cr site of the Cr_2O_3 matrix associated with a certain charge-compensating defect, such as an oxide-ion vacancy or an electron deficiency. A possible mechanism for the stabilization of the iron(II) species at the Cr site is that the ^{57}Mn atoms produced by the $^{54}\text{Cr}(\alpha, p)^{57}\text{Mn}$ reaction were partly in the divalent state, and a part of them remained in the same valence state after β -decay to ^{57}Fe .

Scanning electron microscopy of the sample showed that the sizes of the Cr_2O_3 particles were much less than 30 nm. Its X-ray powder pattern showed a considerable background ascribable to an amorphous phase. The ^{57}Fe atoms arising from ^{57}Mn may have stabilized in the iron(II) state in the amorphous phase with a high density of lattice defects. This is the second possible origin of the observed iron(II) species. Another possibility is a stabilization of ^{57}Fe out of the Cr_2O_3 particles. Since the (α, p) reaction imparts to the ^{57}Mn atoms a recoil energy amounting up to an order of 100 keV, it is possible that some part of the atoms recoiled out of the particles, coming to rest in the binder used to fix the particles to the

target holder. Since the binder is an organic material, it is expected that some part of the ^{57}Fe arising from them took the reduced form.

Recently, Binczycka et al. observed the conversion electron Mössbauer spectrum of ^{57}Fe implanted in $^{56}\text{Fe}_2\text{O}_3$ at room temperature.¹⁹⁾ They observed iron at room temperature in the following states: Substitutional positions of hematite, a magnetite-type structure, a paramagnetic iron(II) state, and a paramagnetic iron(III) state identified as small particles of Fe_2O_3 or Fe_3O_4 . The observed fraction of each state was reported to agree well with the calculated values obtained from the local iron atom enrichment and the phase diagram. The origin of iron(II) state observed in their sample is considered to be different from that of the state observed in our experiment, since in their experiment iron was implanted in a limited region of the surface up to an iron concentration of about 44 at. %.

A clearly split doublet was observed for ^{57}Fe arising from ^{57}Mn in CrO_3 (Fig. 4(c)). The isomer shift indicates high-spin iron(III) ions coordinated with oxide ions. The absence of the iron(II) species is considered to be a proper consequence of the oxidizing characteristic of the matrix.

The crystal structure of CrO_3 comprises infinite chains of corner-sharing CrO_4 tetrahedra running parallel to the crystal axis.²⁰⁾ The large quadrupole splitting observed suggests a site with low local symmetry. An interstitial site is one possibility. Alternatively, the iron(III) ions might replace the chromic ions in the chain, and one or two of the ligand oxide ions might remove to compensate for the smaller positive charge of Fe^{3+} than Cr^{6+} , resulting in a highly asymmetric configuration. Within the experimental uncertainties, no species with valence states exceeding three were detected. Implantation of $^{57}\text{Mn}^{7+}$ ions into a Mn^{7+} compound is expected to give rise to an ^{57}Fe species in unusually high valence states, since they may be stabilized in the Mn^{7+} state and the succeeding β^- -decay may result in an increase in the oxidation number, as described above.

We are thankful to the former staff of the Riken 160 cm cyclotron for irradiations, to Dr. H. Sakairi for his help in electron microscopy, and to Mr. Y. Iimura for X-ray powder pattern measurements.

References

- 1) R. S. Preston and B. J. Zabransky, *Phys. Lett. A*, **55**, 179 (1975).
- 2) E. Browne, J. M. Dairiki, and R. E. Doebler, "Table of Isotopes," 7th ed, ed by C. M. Lederer and V. S. Shirley, Wiley-Interscience, New York (1978), p. 165.
- 3) E. Browne and R. B. Firestone, "Table of Radioactive Isotopes," ed by V. S. Shirley, Wiley-Interscience, New York (1986), p. 56-3.
- 4) E. H. Appelman, *J. Am. Chem. Soc.*, **90**, 1900 (1968).
- 5) G. J. Perlow and M. R. Perlow, *J. Chem. Phys.*, **48**, 955 (1968).

- 6) S. Ambe and F. Ambe, *J. Chem. Phys.*, **63**, 4077 (1975).
 - 7) N. Sakai, *Hyperfine Interact.*, **42**, 1165 (1988).
 - 8) A. H. Muir, Jr., K. J. Ando, and H. M. Coogan, "Mössbauer Effect Data Index 1958—1965," Interscience Publishers, New York (1966), p. 26.
 - 9) H. de Waard and L. Niesen, in "Mössbauer Spectroscopy Applied to Inorganic Chemistry," ed by G. J. Long, Plenum Press, New York (1987), Vol. 2, p. 1.
 - 10) R. E. Newnham and Y. M. de Haan, *Z. Krist.*, **117**, 235 (1962).
 - 11) T. R. McGuire, E. J. Scott, and F. H. Grannis, *Phys. Rev.*, **102**, 1000 (1956).
 - 12) O. C. Kistner and A. W. Sunyar, *Phys. Rev. Lett.*, **4**, 412 (1960).
 - 13) N. N. Greenwood and T. C. Gibb, "Mössbauer Spectroscopy," Chapman and Hall, London (1971), p. 241.
 - 14) R. L. Blake, R. E. Hessevick, T. Zoltai, and L. W. Finger, *Am. Mineral.*, **51**, 123 (1966).
 - 15) T. Birchall and A. F. Reid, *J. Solid State Chem.*, **13**, 351 (1975).
 - 16) K. Ôno and A. Ito, *J. Phys. Soc. Jpn.*, **17**, 1012 (1962).
 - 17) R. E. Vandenberghe, A. E. Verbeeck, E. de Grave, and W. Stiers, *Hyperfine Interact.*, **29**, 1157 (1986).
 - 18) N. N. Greenwood and A. T. Howe, *J. Chem. Soc., Dalton Trans.*, **1972**, 110.
 - 19) H. Binczycka, G. Marest, N. Moncoffre, and J. Stanek, *Hyperfine Interact.*, **56**, 1557 (1990).
 - 20) J. S. Stephens and D. W. J. Cruickshank, *Acta Crystallogr., Sect. B*, **26**, 222 (1970).
-